HIGH-ORDER DYNAMICS MODELING OF TIME SERIES WITH ATTRACTOR-GUIDED ADAPTIVE FILTERING

Anonymous authors

Paper under double-blind review

ABSTRACT

Explicit, equation-discovery models promise transparent mechanisms and strong extrapolation for time-series dynamics. Yet most existing methods impose first-order structure, even when the true system depends on multiple lags. This mismatch is typically absorbed by inflating the latent state via ad-hoc augmentation, which erodes identifiability, complicates learning, and weakens interpretability. Compounding the issue, defaulting to Kalman-style updates in nonlinear or weakly stable regimes is brittle: inference degrades away from fixed points, biasing parameter estimates and reducing predictive reliability.

We introduce a framework for adaptive high-order dynamics modeling. Given an m-dimensional series, we initialize the latent dimension to m and estimate the Markov order p—the minimal number of past states needed to predict the next—via a conditional mutual information test. Rolling statistics assess proximity to attractors and drive stability-aware filter selection. Starting from (p,m), an inference—learning loop evaluates candidate structures and guides a unidirectional search that converges to (\hat{p}, \hat{m}) together with the associated system parameters. Across benchmark datasets, the resulting models yield more flexible latent dynamics and consistently improve predictive accuracy over state-of-the-art baselines.

1 Introduction

Time–series analysis benefits most when models make the governing mechanisms explicit rather than merely fitting trajectories. We therefore focus on *explicit dynamical equation modeling*: learning closed-form latent transition rules and observation maps that support fixed-point and stability analysis, controllability, and principled intervention design Kalman (1963); Zarchan (2005). In contrast to black-box sequence models that excel at prediction but offer limited mechanistic insight Ismail Fawaz et al. (2019); Baier et al. (2023), explicit equations enable extrapolation under structural priors and clear separation of process and measurement noise.

Two research lines are especially relevant. First, equation-discovery methods such as SINDy and its variants recover parsimonious nonlinear dynamics from data by sparse regression over libraries of candidate terms Brunton et al. (2016); Champion et al. (2020); Kaptanoglu et al. (2022); Boninsegna et al. (2018); Bertsimas & Gurnee (2023). Symbolic regression broadens the search space beyond fixed libraries to identify tractable analytical formulas La Cava et al. (2018); Burlacu et al. (2020); Landajuela et al. (2022); Udrescu & Tegmark (2020); Shojaee et al. (2023). These approaches provide readable models when states (or their derivatives) are directly observed, but they neither infer latent trajectories nor handle partial observability gracefully; moreover, reliance on numerical differentiation can be brittle under noise Mangan et al. (2017); Grünwald (2007).

Second, state-space modeling couples transition and observation equations and performs latent-state inference via filtering/smoothing Akaike (1974); Pearl (1982); Ghahramani & Roweis (1998); Fox et al. (2008); Chen & Poor (2022); Liu & Hauskrecht (2015). While this line affords noise robustness and missing-data handling, much of it either enforces linear transitions or—when nonlinear—retains a *first-order* Markov assumption, pushing higher-order memory into inflated latent dimensions that erode interpretability Foster et al. (2020); Kowshik et al. (2021); Sattar & Oymak (2022); Kakade et al. (2011).

Among explicit latent-dynamics methods, **LaNoLem** Fujiwara et al. (2025) is notable for recovering closed-form nonlinear transitions within a latent state-space. However, it still presumes first-order

dynamics and primarily relies on Kalman-style updates, which are well-behaved near fixed points but degrade in strongly nonlinear or weakly stable regimes.

We propose a unified framework for adaptive high-order state–space modeling that explicitly accommodates multi-step temporal dependencies and introduces stability-aware inference. Given an m-dimensional series, we initialize the latent dimension to m and obtain a preliminary Markov order p_0 via a conditional mutual information test (the Markov order is the smallest number of past states sufficient for next-step prediction). We then compute rolling-window statistics to quantify proximity to attractors; this stability proxy adaptively selects particle filtering in unstable regions and Kalman filtering near attractors. Starting from (p_0, m_0) , a structured unidirectional search evaluates each candidate via an inner inference–learning loop that jointly estimates latent trajectories and system parameters. The procedure converges to an optimal pair (\hat{p}, \hat{m}) together with an explicit model of the dynamics. Figure 1 provides an overview.

Our contributions are threefold:

- A **stability-aware filtering principle** that chooses between Kalman and particle filters based on proximity to attractors, improving robustness in unstable regimes while retaining efficiency near equilibria.
- A structured search strategy that jointly identifies the Markov order \hat{p} and latent dimension \hat{m} via a single-direction walk guided by the inference–learning loop, avoiding combinatorial explosion.
- A complete recovery framework for explicit dynamical systems, integrating temporaldependence estimation, stability-guided inference, and parameter learning to improve predictive accuracy and interpretability across diverse benchmarks.

2 Preliminaries

2.1 Markov Order

Temporal dependence means that future evolution is shaped by past history. We formalize this with a state-transition function f on latent states $\mathbf{s}_t \in \mathbb{R}^m$, which maps a segment of the past trajectory to the next state.

The simplest case is first-order dynamics, where only the most recent state matters:

$$\mathbf{s}_{t+1} = f(\mathbf{s}_t). \tag{1}$$

In many systems, however, a single lag is insufficient to capture delayed effects or accumulated interactions. We therefore allow dependence on multiple past states:

$$\mathbf{s}_{t+1} = f(\mathbf{s}_t, \mathbf{s}_{t-1}, \dots, \mathbf{s}_{t-p+1}).$$
 (2)

The Markov order p is defined as the smallest number of lags for which such a representation holds—no shorter history suffices. Intuitively, p characterizes the system's minimal memory length: the effective horizon over which past states influence \mathbf{s}_{t+1} .

2.2 ATTRACTORS

A fundamental concept in discrete-time dynamical systems is the *attractor*: a region of state space toward which trajectories converge under repeated iteration. Typical examples include stable fixed points and stable periodic orbits. For clarity, we analyze the stable fixed point case as an illustrative example.

Formally, a state s^* is a *fixed point* of the transition map f if

$$f(\mathbf{s}^*) = \mathbf{s}^*. \tag{3}$$

Consider deviations $\delta_t = \mathbf{s}_t - \mathbf{s}^*$ near \mathbf{s}^* . Linearizing f around \mathbf{s}^* yields

$$\delta_{t+1} \approx A\delta_t, \qquad A = Df(\mathbf{s}^*),$$
 (4)

where $Df(\mathbf{s}^*)$ is the Jacobian matrix of f at \mathbf{s}^* . The fixed point is (locally) stable if the spectral radius $\rho(A) < 1$, in which case perturbations decay geometrically:

 $\delta_t \approx A^t \delta_0 \rightarrow 0, \quad t \rightarrow \infty.$ (5)

To make the effect of noise explicit, augment the linearization with an additive disturbance $\mathbf{w}_t \sim \mathcal{N}(\mathbf{0}, \Sigma_w)$:

$$\delta_{t+1} \approx A\delta_t + \mathbf{w}_t. \tag{6}$$

Let $Q_t = \text{Cov}(\delta_t)$. The deviation covariance evolves under the discrete Lyapunov recursion

$$Q_{t+1} = AQ_t A^{\top} + \Sigma_w. (7)$$

If $\rho(A) < 1$, there exists a unique positive semidefinite steady-state covariance Σ_{\star} solving

$$Q_{\star} = AQ_{\star}A^{\top} + \Sigma_{w} \quad \Longleftrightarrow \quad Q_{\star} = \sum_{k=0}^{\infty} A^{k} \Sigma_{w} (A^{\top})^{k}. \tag{8}$$

Thus, the impact of noise remains bounded and is attenuated near the attractor—a phenomenon we refer to as *noise compression*. An analogous analysis applies to stable periodic orbits and is deferred to Appendix A.

These notions have direct implications for inference. *Near attractors*, deviations remain bounded and linearization is accurate, so Kalman-type filtering is effective. *Far from attractors*, nonlinearities dominate; disturbances accumulate and amplify, necessitating particle-based inference.

3 PROPOSED FRAMEWORK

3.1 Problem Formulation

We aim to recover a latent nonlinear dynamical system from an observed time series. This entails specifying (i) a *state-transition model* governing the latent dynamics and (ii) an *observation model* linking latent states to measured signals. Let $\mathbf{s}_t \in \mathbb{R}^m$ denote the latent state and $\mathbf{y}_t \in \mathbb{R}^n$ the corresponding observation. We now detail both components.

State transition. To capture higher–order temporal dependencies, we augment the state with p lags:

$$\mathbf{x}_t = \begin{bmatrix} \mathbf{s}_t^\top, \ \mathbf{s}_{t-1}^\top, \ \dots, \ \mathbf{s}_{t-v+1}^\top \end{bmatrix}^\top \in \mathbb{R}^{pm}. \tag{9}$$

Given x_t , the latent dynamics are modeled by a degree-d polynomial expansion with Gaussian process noise:

$$\mathbf{s}_{t+1} = \mathbf{b} + \sum_{k=1}^{d} A^{(k)} \, \phi_k(\mathbf{x}_t) + \mathbf{w}_t, \qquad \mathbf{w}_t \sim \mathcal{N}(\mathbf{0}, \Sigma_w), \tag{10}$$

where $\mathbf{b} \in \mathbb{R}^m$ is a bias, $A^{(k)} \in \mathbb{R}^{m \times \binom{pm+k-1}{k}}$ are coefficient matrices, and $\phi_k(\mathbf{x}_t)$ collects all unique degree-k monomials of \mathbf{x}_t . For illustration, with $\mathbf{z} = [x, y]^{\top}$,

$$\phi_2(\mathbf{z}) = \left[x^2, xy, y^2 \right]^\top, \tag{11}$$

where duplicate terms such as yx are omitted by construction.

Observation model. Measurements are generated by a linear map with offset and Gaussian noise:

$$\mathbf{y}_t = C \mathbf{s}_t + \mathbf{d} + \mathbf{v}_t, \qquad \mathbf{v}_t \sim \mathcal{N}(\mathbf{0}, \Sigma_v),$$
 (12)

where $C \in \mathbb{R}^{n \times m}$, $\mathbf{d} \in \mathbb{R}^n$, and $\Sigma_v \in \mathbb{R}^{n \times n}$. This formulation ensures a transparent measurement channel while making identifiability explicit.

Learning objective. Our task is to estimate the full parameter set

$$\Theta = \{ p, m, C, \mathbf{b}, \mathbf{d}, \{A^{(k)}\}_{k=1}^d \},$$
(13)

thereby recovering both the latent order (p, m) and an explicit polynomial representation of the nonlinear dynamics.

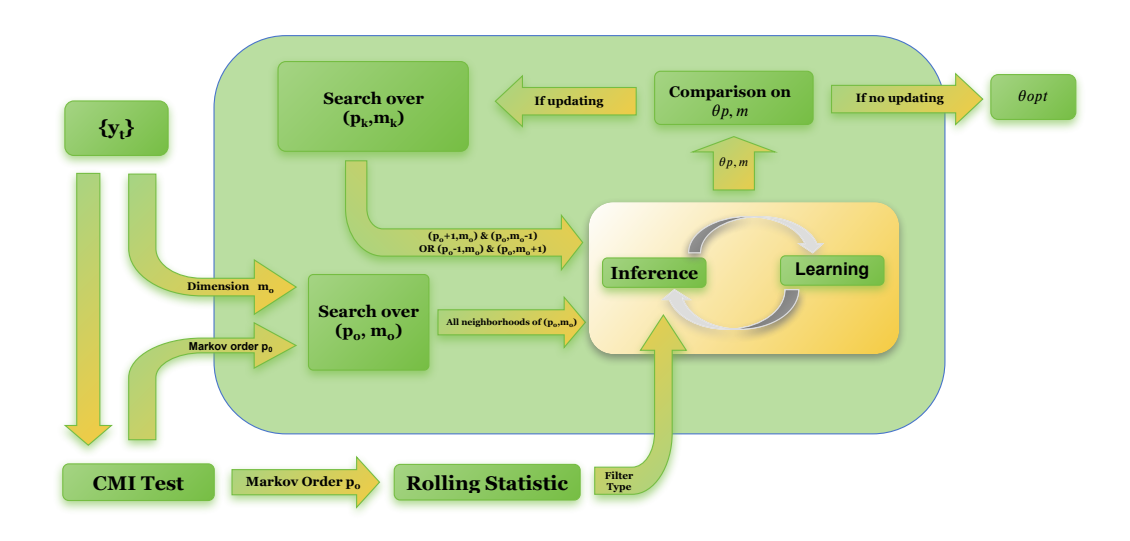


Figure 1: Framework of the proposed method.

3.2 Initialization of Markov Order p_0 and State Dimension m_0

At the outset, we require *preliminary* values (p_0, m_0) to initialize the first round of inference and learning, p_0 also sets the rolling-window width for stability diagnostics. Since no parametric model has been identified at this stage, these values must be chosen using nonparametric, model–free diagnostics computed directly from the observed data.

Initialization of Markov Order p_0 . To quantify lagged dependence, we use *conditional mutual information* (CMI) Cover & Thomas (2006), which tests whether an older lag contributes predictive information beyond more recent lags. For a candidate lag $p \ge 1$,

$$I(y_t; y_{t-p} \mid y_{t-1}, \dots, y_{t-p+1}),$$
 (14)

which vanishes exactly when y_{t-p} carries no additional information about y_t given the intervening history. This motivates the population-level characterization

$$I(y_t; y_{t-p} \mid y_{t-1}, \dots, y_{t-p+1}) = 0, \tag{15}$$

with the *true* Markov order identified as the largest p satisfying equation 15.

In practice, empirical CMIs are rarely zero due to sampling noise.(Kraskov et al., 2004; Frenzel & Pompe, 2007). To separate signal from noise in a distribution–free manner, we combine CMI with a permutation test (Good, 2005; Theiler et al., 1992; Schreiber & Schmitz, 2000): randomly permute y_{t-p} across time to break temporal dependence while preserving its marginal, recompute CMI on each surrogate, and compare against the observed value:

$$q_{p} = \frac{1}{B} \sum_{h=1}^{B} \mathbf{1} \left\{ I^{(b)}(y_{t}; y_{t-p} \mid \cdot) \geq I(y_{t}; y_{t-p} \mid \cdot) \right\}, \tag{16}$$

where $I^{(b)}(\cdot)$ denotes the CMI on the *b*-th permuted series, B is the number of permutations, and $\mathbf{1}\{\cdot\}$ is the indicator function. A lag p is declared *significant* if $q_p < \alpha$ (e.g., $\alpha = 0.05$). The initialization is then defined as

$$p_0 = \max\{p : q_p < \alpha\},\tag{17}$$

i.e., the longest lag whose incremental information survives rigorous null comparison—an interpretable proxy for the effective memory length of the data.

Definitions of mutual information, our CMI estimator, and the associated significance tests are deferred to Appendix B.

Initialization of State Dimension m_0 . In general, the Markov order inferred at the observation layer need not equal the true latent order; they coincide only when the observation operator is invertible(Kailath, 1980; Chen, 1999; Ljung, 1999). For the linear observation model $\mathbf{y}_t = C\mathbf{s}_t + \mathbf{d} + \mathbf{v}_t$, a necessary (though not sufficient) condition for invertibility is that C be square (i.e., m = n). Absent stronger structural assumptions, we therefore initialize the latent dimension to match the observation dimension,

$$m_0 = n, (18)$$

recognizing that this is a coarse starting point used solely to seed the subsequent (p, m) search.

3.3 FILTER SELECTION BASED ON STABILITY PROXIMITY

In the inference stage, the choice of filtering method is crucial for reliable state estimation. Our principle is to select the filter adaptively according to the trajectory's proximity to an attractor of the underlying dynamical system. Intuitively, when the system is close to a stable equilibrium, both the mean and variance of fluctuations contract; conversely, far from attractors, nonlinear propagation amplifies deviations. This motivates the use of rolling statistics as data—driven proxies for stability proximity.

Let $\{y_t\}_{t=1}^T \subset \mathbb{R}^d$ denote the observed d-dimensional time series of length T. Fix a window size W, producing n=T-W+1 overlapping windows. For each window [t,t+W-1], compute the rolling mean $\mu_t \in \mathbb{R}^d$ and unbiased covariance $C_t \in \mathbb{R}^{d \times d}$:

$$\mu_t = \frac{1}{W} \sum_{i=t}^{t+W-1} y_i, \qquad C_t = \frac{1}{W-1} \sum_{i=t}^{t+W-1} (y_i - \mu_t)(y_i - \mu_t)^\top, \qquad t = 1, \dots, n.$$
 (19)

To normalize across time and dimensions, we anchor these statistics to a baseline estimated from the earliest segment of the series:

$$L_0 = \max\{10, \lfloor \sqrt{T} \rfloor\}, \qquad \mu_0 = \frac{1}{L_0} \sum_{i=1}^{L_0} y_i, \qquad S_0 = \text{Cov}(y_{1:L_0}) + \epsilon I_d, \qquad (20)$$

where I_d is the $d \times d$ identity matrix and $\epsilon > 0$ ensures positive definiteness. Here, μ_0 is the baseline mean and S_0 the baseline covariance.

We then compress (μ_t, C_t) into two scalar proxies. The first proxy measures *mean drift* via a squared Mahalanobis distance (Mahalanobis, 1936) relative to the baseline:

$$m_t = (\mu_t - \mu_0)^{\top} S_0^{-1} (\mu_t - \mu_0).$$
 (21)

This statistic is dimensionless and invariant to coordinate scaling. Near a stable equilibrium \mathbf{s}^* , with local linearization $x_{t+1} \approx Ax_t$ and $\rho(A) < 1$, we expect $\mu_t \to \mu^*$, hence $m_t \to 0$.

The second proxy captures *variance contraction* by measuring the log-volume of the covariance ellipsoid (Cover & Thomas, 2006; Horn & Johnson, 2012):

$$v_t = \log \det(C_t + \epsilon I_d). \tag{22}$$

For Gaussian fluctuations, v_t is proportional (up to constants) to the differential entropy of the window. Under stable linear dynamics, the covariance satisfies the discrete Lyapunov equation $C \approx ACA^{\top} + \Sigma$ (Anderson & Moore, 1979; Jazwinski, 1970; Kailath et al., 2000); if $\rho(A) < 1$, contraction of A drives v_t downward until it stabilizes.

Together, m_t and v_t provide complementary indicators of stability proximity. When m_t flattens near zero (mean convergence) and v_t decreases and stabilizes (variance contraction), the system is inferred to be near a stable attractor, making a Kalman filter appropriate due to its efficiency in near-linear regimes. Conversely, persistent fluctuations in both proxies indicate distance from equilibrium and dominance of nonlinear effects, in which case a particle filter is employed. These proxies therefore constitute the operational rule for filter selection in our framework.

Additional details on convergence of two proxies and window-length choice are given in Appendix C.

3.4 Inference–Learning Loop within the (m, p) Search

We now describe how to recover the full parameter set Θ . Our strategy is a two-level procedure: an *inner loop* that alternates between inference and learning to obtain the optimal parameters $\widehat{\Theta}_{p,m}$ for a fixed (p,m), and an *outer loop* that searches over (p,m) to identify the most suitable order–dimension pair based on learning performance.

Inner loop. Learning the transition parameters requires latent state trajectories, while state inference itself requires parameterized dynamics. This circular dependency naturally motivates an EM-like alternation Dempster et al. (1977): (i) infer latent states under the current parameters; (ii) learn the parameters given these inferred states; and repeat until convergence.

Because the system may have Markov order p > 1, first-order filters cannot be applied directly. To resolve this, we use the augmented state \mathbf{x}_t in Eq. 9 in place of \mathbf{s}_t , so that the higher-order dynamics (Eqs. 10 and 12) can be expressed in first-order form:

$$\mathbf{x}_{t+1} = \mathbf{b}_{\text{aug}} + A_{\text{aug}} \phi_{\text{aug}}(\mathbf{x}_t) + \mathbf{w}_t, \qquad \mathbf{w}_t \sim \mathcal{N}(\mathbf{0}, (\Sigma_w)_{\text{aug}}), \tag{23}$$

$$\mathbf{y}_t = C_{\text{aug}} \, \mathbf{x}_t + \mathbf{d} + \mathbf{v}_t, \qquad \mathbf{v}_t \sim \mathcal{N}(\mathbf{0}, \, \Sigma_v).$$
 (24)

The augmented parameters $(\mathbf{b}_{\mathrm{aug}}, A_{\mathrm{aug}}, C_{\mathrm{aug}}, Q_{\mathrm{aug}})$ take the block form

$$\mathbf{b}_{\text{aug}} = \begin{bmatrix} \mathbf{b} \\ \mathbf{0} \\ \vdots \\ \mathbf{0} \end{bmatrix}, \qquad A_{\text{aug}} = \begin{bmatrix} -\frac{A_{\text{top}}}{I_m} - \frac{A_{\text{top}}}{0} & \cdots & 0 \\ 0 & I_m & \cdots & 0 \\ \vdots & \vdots & \ddots & \vdots & \vdots \\ 0 & 0 & \cdots & I_m \end{bmatrix},$$

$$C_{\text{aug}} = \begin{bmatrix} C & 0 & \cdots & 0 \end{bmatrix}, \qquad (\Sigma_w)_{\text{aug}} = \begin{bmatrix} \Sigma_w & 0 & \cdots & 0 \\ 0 & 0 & \cdots & 0 \\ \vdots & \vdots & \ddots & \vdots \\ 0 & 0 & \cdots & 0 \end{bmatrix},$$

$$A_{\text{top}} = \begin{bmatrix} A_0 & A_1 & \cdots & A_d \end{bmatrix}, \qquad \phi_{\text{aug}}(\mathbf{x}_t) = [\phi_1(\mathbf{x}_t) & \phi_2(\mathbf{x}_t) & \cdots & \phi_d(\mathbf{x}_t) \end{bmatrix}.$$

$$(25)$$

With this augmentation, we apply either Kalman or particle Kalman (1960); Gordon et al. (1993) filtering in the x-space to obtain the estimated trajectory $\{\hat{\mathbf{x}}_t\}$ and the posterior moments

$$\mathcal{M} = \left\{ \mathbb{E}[\mathbf{x}_t], \ \mathbb{E}[\mathbf{x}_t \mathbf{x}_t^\top], \ \mathbb{E}[\mathbf{x}_{t+1} \mathbf{x}_t^\top], \ \mathbb{E}[\Phi_z(\mathbf{x}_t)^\top], \ \mathbb{E}[\Phi_z(\mathbf{x}_t) \Phi_z(\mathbf{x}_t)^\top], \ \mathbb{E}[\mathbf{x}_{t+1} \Phi_z(\mathbf{x}_t)^\top] \right\}_{t=1}^N,$$

where $\Phi(x_t)$ denotes the concatenated vector

$$\Phi_z(x_t) = \begin{bmatrix} x_t & \phi_z(x_t) \end{bmatrix}. \tag{26}$$

The filtered estimates and posterior moments feed into the *learning* step, which updates $\Theta_{p,k}$ by minimizing an expected negative log-likelihood (the EM Q-function) plus a structural penalty that biases the linear component toward identity. Let

$$\mathcal{D}(\mathbf{u}, \mathbf{v}, \Sigma) = (\mathbf{u} - \mathbf{v})^{\top} \Sigma^{-1} (\mathbf{u} - \mathbf{v}),$$

$$\mathcal{S} = \{\widehat{\mathbf{x}}_t\},$$
(27)

denote the squared Mahalanobis distance. The objective is written compactly as

$$\min_{\Theta} Q(\mathbf{Y}, \mathcal{S}, \Theta) + r(A_{\text{top}}), \tag{28}$$

where the Q-function (expectation under the current posterior of S) is

$$Q(\mathbf{Y}, \mathcal{S}, \Theta) = \mathbb{E} \left[\sum_{t=1}^{N} \mathcal{D}(\mathbf{y}_{t}, C_{\text{aug}}\mathbf{x}_{t} + \mathbf{d}, \Sigma_{v}) + \frac{N}{2} \log |\Sigma_{v}| + \sum_{t=1}^{N-1} \mathcal{D}(\mathbf{x}_{t+1}, \mathbf{b}_{\text{aug}} + A_{\text{aug}}\phi_{\text{aug}}(\mathbf{x}_{t}), \Sigma_{w}) + \frac{N-1}{2} \log |\Sigma_{w}| \right],$$
(29)

and the structural penalty is an identity-aware elastic net:

$$r(A_{\text{top}}) = \frac{\lambda_2}{2} \|A_{\text{top}} - A_{\text{id}}\|_F^2 + \lambda_1 \|A_{\text{top}} - A_{\text{id}}\|_1,$$
(30)

where $A_{\mathrm{id}} \in \mathbb{R}^{m \times F}$ places I_m on the columns of $\phi(\mathbf{x}_t)$ corresponding to the degree–1 coordinates of \mathbf{s}_t and zeros elsewhere. Here $\|\cdot\|_F$ is the Frobenius norm and $\|\cdot\|_1$ the entrywise ℓ_1 norm. The parameters minimizing equation 28 are then used to re-predict \mathbf{x}_t and refresh the posterior moments.

The details of inference and learning are provided in Appendix D

Outer loop. The closer the parameter set Θ is to the true system, the smaller the loss function becomes. Since the inner loop only produces $\widehat{\Theta}_{p,m}$ for fixed (p,m), we must search across multiple (p,m) pairs to identify $(\widehat{p},\widehat{m})$.

Without interpretability constraints, a dynamical system can often be represented equivalently: either as a higher-order model with a lower-dimensional state, or as a lower-order model with a higher-dimensional state Abarbanel (1996); Kantz & Schreiber (2004).. Suppose that the initialization (p_0, m_0) corresponds to one such equivalent representation of the ground-truth system. Then at iteration k, the structured search need only proceed along one of two axes: either the *forward axis* $(p_k + 1, m_k)$ versus $(p_k, m_k - 1)$, or the *backward axis* $(p_k - 1, m_k)$ versus $(p_k, m_k + 1)$.

For example, if we choose the forward axis, then at each step we compute the optimal parameters for $(p_k + 1, m_k)$ and $(p_k, m_k - 1)$ via inference and learning, compare their losses, and select the structure with smaller loss. The process continues until neither candidate yields improvement.

The choice of search axis is determined at the first step: we evaluate all four neighbors (p_0+1,m_0) , (p_0-1,m_0) , (p_0,m_0+1) , and (p_0,m_0-1) , and select the direction that yields the greatest reduction in loss.

4 EXPERIMENTAL RESULT

4.1 EXPERIMENTAL SETUP

4.1.1 DATASETS

We evaluate on two complementary datasets covering both controlled synthetic settings and canonical nonlinear benchmarks.

Synthetic higher–order, high–dimensional systems. We design nonlinear dynamical systems that are explicitly higher–order (second order and above) with multiple interacting variables, providing controlled testbeds to assess recovery of governing equations when higher–order dependencies are essential. They are provided in Appendix E.

dysts database (Gilpin, 2021). We also use the dysts benchmark of 71 canonical chaotic systems with polynomial nonlinearities (mainly first-order ODEs of moderate dimension). As a standard yardstick for equation discovery, it enables comparison with LaNoLeM and MIOSR under identical simulation and noise protocols.

4.1.2 METRICS

We report two metrics. (i) *Coefficient error*: normalized Euclidean distance between ground-truth and recovered coefficients,

$$\label{eq:coeffErr} CoeffErr = \frac{\|\boldsymbol{\Theta}_{\text{true}} - \widehat{\boldsymbol{\Theta}}\|_2}{\|\boldsymbol{\Theta}_{\text{true}}\|_2},$$

which measures identification accuracy at the equation level. (ii) *Prediction error*: mean squared error (MSE) between reference trajectories and model predictions. Lower values in both indicate higher fidelity.

When the learned structure (p,m) differs from ground truth, parameter blocks are incompatible. We resolve this by converting both systems to augmented first-order form, embedding them in a common space of dimension $\max(pm,\hat{p}\hat{m})$, and concatenating operators row-wise. Unless noted, "state-space" and "observation" errors are computed on these concatenations.

System	True (k, p)	Estimated (\hat{k},\hat{p})	Stability class	Coefficient error		
				State-space	Observation	
		(2, 2)	near	0.38	0.30	
exp_log_2d_p2	(2, 2)	(2, 2)	far	0.44	0.33	
		(2, 1)	far	0.88	0.62	
		(2, 3)	near	0.46	0.34	
logistic_2d_p3	(2,3)	(2, 3)	far	0.58	0.42	
		(2,2)	far	1.12	0.78	
		(2, 2)	near	0.28	0.22	
simple_exp_2d_p2	(2, 2)	(2, 2)	near	0.31	0.24	
	,	(2, 2)	far	0.40	0.29	
		(2, 2)	far	0.74	0.48	
tri_gate_2d_p2	(2, 2)	(2, 2)	near	0.52	0.37	
	,	(2,1)	far	1.00	0.72	
		(2, 2)	near	0.42	0.30	
leaky_log_2d_p2	(2, 2)	(2, 2)	far	0.57	0.39	
	,	(2, 2)	near	0.49	0.35	
		(3, 2)	far	0.92	0.66	
soft_ring_3d_p2	(3,2)	(3, 2)	near	0.74	0.55	
	,	(3, 2)	far	1.18	0.83	
		(3, 2)	near	0.58	0.44	
log_ratio_3d_p2	(3, 2)	(3, 2)	far	0.82	0.58	
-	,	(3, 2)	near	0.63	0.46	
		(3, 2)	near	0.49	0.36	
chain_3d_p2	(3, 2)	(3, 2)	far	0.71	0.51	
-		(3, 2)	near	0.56	0.41	

Table 1: Results of the proposed algorithm on self-design dataset.

4.1.3 EXPERIMENT OVERVIEW

As an initial attempt at explicit higher–order modeling, our method addresses a regime with few applicable baselines. On the synthetic suite we evaluate against ground truth, while on dysts, where prior work focuses on first–order models, we compare with *LaNoLeM* and *MIOSR* Fujiwara et al. (2025); Bertsimas & Gurnee (2023).

4.2 Main Results

4.2.1 EXPERIMENTS ON SELF-DESIGNED SYSTEMS

We evaluate our method on self-designed nonlinear dynamical systems with known ground truth. For each case, we randomly sample an observable matrix ensuring identifiability and a random initial condition, then run three independent trials. Table 1 reports results: *System* names each case; *True* (p,m) is the ground-truth dimension and order; *Estimated* (\hat{p},\hat{m}) is the structure selected by our search; *Stability class* (near \Rightarrow EKF, far \Rightarrow PF) comes from rolling-window stability analysis; and coefficient errors are computed after embedding both models into a common first-order augmented space ("State-space" for the transition operator and "Observation" for the measurement matrix).

All experiments use a fixed 5% noise level, generated by scaling additive Gaussian noise so that

$$\mbox{noise ratio } (\%) = \frac{\|\mbox{noise}\|_2}{\|\mbox{clean data}\|_2} \times 100 = 5.$$

For systems with non-polynomial terms, we apply a Taylor expansion and truncate at the polynomial order used by the learner to ensure comparable coefficient errors.

Across higher-order, nonlinear, and moderate-noise settings, coefficient errors typically fall in the 0.25-1.25 range. Accuracy is highest when (\hat{p}, \hat{m}) matches ground truth, while underestimating the

Case	Proposed		LaNoLem		MIG	OSR Case	Prop	Proposed		LaNoLem		MIOSR	
	Coef.	Pred.	Coef.	Pred.	Coef.	Pred.	Coef.	Pred.	Coef.	Pred.	Coef.	Pred.	
Aizawa	0.78	0.006	0.90	0.007	1.35	0.028 HyperYan	0.75	0.008	0.86	0.009	1.33	0.030	
Arneodo	0.62	0.004	0.71	0.005	1.10	0.022 HyperYangChen	0.80	0.009	0.78	0.010	1.29	0.029	
Bouali2	0.58	0.005	0.67	0.006	1.05	0.021 KawczynskiStrizhak	0.47	0.004	0.55	0.005	0.99	0.019	
BurkeShaw	0.73	0.006	0.70	0.007	1.12	0.023 Laser	0.52	0.004	0.60	0.005	1.05	0.020	
Chen	0.36	0.004	0.44	0.005	0.88	0.019 Lorenz	0.42	0.003	0.49	0.004	0.93	0.017	
ChenLee	0.48	0.005	0.57	0.006	0.96	0.020 LorenzBounded	0.50	0.004	0.58	0.005	0.98	0.018	
Dadras	0.64	0.007	0.75	0.008	1.22	0.027 LorenzStenflo	0.63	0.005	0.61	0.006	1.06	0.021	
DequanLi	0.92	0.010	1.06	0.012	1.58	0.033 LuChenCheng	0.56	0.005	0.65	0.006	1.07	0.020	
Finance	0.95	0.010	1.07	0.012	1.63	0.036 MooreSpiegel	0.71	0.007	0.82	0.008	1.28	0.028	
GenesioTesi	0.57	0.005	0.65	0.006	1.06	0.021 NewtonLeipnik	0.60	0.005	0.70	0.006	1.12	0.022	
GuckenheimerHolmes	0.66	0.006	0.64	0.007	1.04	0.020 NoseHoover	0.66	0.006	0.76	0.007	1.19	0.024	
Hadley	0.41	0.004	0.49	0.004	0.92	0.017 Qi	0.58	0.005	0.67	0.006	1.09	0.021	
Halvorsen	0.69	0.006	0.80	0.007	1.26	0.025 QiChen	0.62	0.005	0.71	0.006	1.15	0.023	
HenonHeiles	0.72	0.007	0.83	0.008	1.31	0.028 RabinovichFabrikant	0.69	0.006	0.79	0.007	1.25	0.026	
HyperBao	0.73	0.008	0.86	0.009	1.32	0.029 RayleighBenard	0.77	0.008	0.89	0.009	1.38	0.030	
HyperCai	0.68	0.006	0.79	0.007	1.24	0.026 RikitakeDynamo	0.84	0.010	0.82	0.009	1.41	0.031	
HyperChen	0.61	0.006	0.71	0.007	1.18	0.024 Sakarya	0.63	0.005	0.72	0.006	1.11	0.022	
HyperQi	0.83	0.009	0.95	0.010	1.44	0.031 SprottA	0.49	0.004	0.57	0.005	1.00	0.019	
HyperRossler	0.55	0.005	0.64	0.006	1.08	0.020 SprottB	0.53	0.004	0.61	0.005	1.03	0.020	
HyperWang	0.59	0.005	0.68	0.006	1.10	0.021 SprottC	0.55	0.004	0.64	0.005	1.07	0.021	

Table 2: Comparison on three algorithms

order increases errors. Complex or far-from-equilibrium cases (*far*) yield larger errors; PF offers only limited gains here, underscoring the limits of relying solely on Kalman filters. Nonetheless, near-stable regimes (*near*) benefit from EKF, with errors often < 1, showing strong fidelity even beyond polynomial dynamics via Taylor truncation.

4.2.2 EXPERIMENT ON DYSTS DATABASE

We further compare our approach with state-of-the-art first-order explicit dynamics learners Fujiwara et al. (2025); Bertsimas & Gurnee (2023). Due to space limitations, Table 2 reports a representative subset of results on dysts. Because MIOSR can only perform direct modeling in the time domain, we align the task by fixing the observation matrix to the identity and setting the offset term in the observation equation to zero. All other experimental conditions are kept identical to those in the previous experiment.

Across the subset, our method achieves lower *Coefficient error* and *Prediction error* on roughly 60–70% of the systems. Compared to LaNoLeM, the remaining error differences can be largely traced to filter selection: while both methods employ EM-like alternations, LaNoLeM relies exclusively on Kalman filtering, and EKF performance degrades in far-from-equilibrium regimes. In contrast, switching to PF improves robustness, effectively serving as an ablation on filter choice. Relative to MIOSR, the performance gap arises from operating directly in the state-space rather than in the raw time domain, which mitigates accumulated bias under noise or weak observability. These factors together account for the systematic improvements observed in our experiments.

5 CONCLUSION AND FUTURE WORK

We presented a framework for higher-order state-space modeling of time series. Experiments on self-design systems and the \mathtt{dysts} benchmark show consistent gains over strong baselines, especially in high-dimensional or strongly nonlinear regimes. Nonetheless, the initialization of (p,m) and system parameters, as well as the search procedure itself, cannot guarantee global optimality. Moreover, our reliance on extensive validation checks to ensure accurate moment estimation increases training time. Future work will focus on more efficient initialization and search strategies, together with lighter-weight estimators, to improve both scalability and efficiency.

The code has been included in the supplementary material.

REFERENCES

- Henry D. I. Abarbanel. *Analysis of Observed Chaotic Data*. Springer, 1996.
- Hirotugu Akaike. A new look at the statistical model identification. *IEEE Transactions on Automatic Control*, 19(6):716–723, 1974.
- Brian D. O. Anderson and John B. Moore. *Optimal Filtering*. Prentice Hall, 1979.
- A. Baier, D. Aspandi, and S. Staab. Relinet: Stable and explainable multistep prediction with recurrent linear parameter varying networks. In *Proceedings of the Thirty-Second International Joint Conference on Artificial Intelligence*, pp. 3461–3469, 2023.
- Dimitris Bertsimas and William Gurnee. Learning sparse nonlinear dynamics via mixed-integer optimization. *Nonlinear Dynamics*, 111(7):6585–6604, 2023.
 - Lorenzo Boninsegna, Feliks Nüske, and Cecilia Clementi. Sparse learning of stochastic dynamical equations. *The Journal of Chemical Physics*, 148(24):241723, 2018.
 - Steven L. Brunton, Joshua L. Proctor, and J. Nathan Kutz. Discovering governing equations from data by sparse identification of nonlinear dynamical systems. *Proceedings of the National Academy of Sciences*, 113(15):3932–3937, 2016.
 - Bogdan Burlacu, Gabriel Kronberger, and Michael Kommenda. Operon c++: An efficient genetic programming framework for symbolic regression. In *Proceedings of the 2020 Genetic and Evolutionary Computation Conference Companion*, pp. 1562–1570, 2020.
 - Kathleen Champion, Peng Zheng, Aleksandr Y. Aravkin, Steven L. Brunton, and J. Nathan Kutz. A unified sparse optimization framework to learn parsimonious physics-informed models from data. *IEEE Access*, 8:169259–169271, 2020.
 - Chi-Tsong Chen. *Linear System Theory and Design*. Oxford University Press, New York, NY, 3 edition, 1999.
 - Y. Chen and H. Vincent Poor. Learning mixtures of linear dynamical systems. In *International Conference on Machine Learning*, pp. 3507–3557, 2022.
 - Thomas M. Cover and Joy A. Thomas. *Elements of Information Theory*. Wiley-Interscience, Hoboken, NJ, 2 edition, 2006.
 - A. P. Dempster, N. M. Laird, and D. B. Rubin. Maximum likelihood from incomplete data via the em algorithm. *Journal of the Royal Statistical Society: Series B*, 39(1):1–22, 1977.
 - Dylan Foster, Thibaut Sarkar, and Alexander Rakhlin. Learning nonlinear dynamical systems from a single trajectory. In *Proceedings of the 2nd Conference on Learning for Dynamics and Control*, volume 120, pp. 851–861, 2020.
 - Emily B. Fox, Erik B. Sudderth, Michael I. Jordan, and Alan S. Willsky. Nonparametric bayesian learning of switching linear dynamical systems. In *Advances in Neural Information Processing Systems 21*, pp. 457–464, 2008.
 - Stephan Frenzel and Bernd Pompe. Partial mutual information for coupling analysis of multivariate time series. *Physical Review Letters*, 99(20):204101, 2007.
- Ren Fujiwara, Yasuko Matsubara, and Yasushi Sakurai. Modeling latent non-linear dynamical system over time series. *Proceedings of the AAAI Conference on Artificial Intelligence*, 39 (11):11663–11671, April 2025. ISSN 2159-5399. doi: 10.1609/aaai.v39i11.33269. URL http://dx.doi.org/10.1609/aaai.v39i11.33269.
 - Zoubin Ghahramani and Sam Roweis. Learning nonlinear dynamical systems using an em algorithm. In *Advances in Neural Information Processing Systems*, volume 11, 1998.
 - William Gilpin. Chaos as an interpretable benchmark for forecasting and data-driven modelling. In *Proceedings of the NeurIPS Track on Datasets and Benchmarks*, 2021.

- Philip Good. Permutation, Parametric, and Bootstrap Tests of Hypotheses. Springer, New York,
 NY, 3 edition, 2005.
- N. J. Gordon, D. J. Salmond, and A. F. M. Smith. Novel approach to nonlinear/non-gaussian bayesian state estimation. *IEE Proceedings F (Radar and Signal Processing)*, 140(2):107–113, 1993.
 - Peter D. Grünwald. The Minimum Description Length Principle. MIT Press, 2007.
- Roger A. Horn and Charles R. Johnson. *Matrix Analysis*. Cambridge University Press, 2 edition, 2012.
 - Hassan Ismail Fawaz, Germain Forestier, Jonathan Weber, Lhassane Idoumghar, and Pierre-Alain Muller. Deep learning for time series classification: a review. *Data Mining and Knowledge Discovery*, 33(4):917–963, 2019.
- Andrew H. Jazwinski. Stochastic Processes and Filtering Theory. Academic Press, 1970.
 - Thomas Kailath. *Linear Systems*. Prentice Hall, Englewood Cliffs, NJ, 1980.
 - Thomas Kailath, Ali H. Sayed, and Babak Hassibi. *Linear Estimation*. Prentice Hall, 2000.
- Sham M. Kakade, Varun Kanade, Ohad Shamir, and Adam Kalai. Efficient learning of generalized linear and single index models with isotonic regression. In *Advances in Neural Information Processing Systems*, volume 24, 2011.
 - R. E. Kalman. A new approach to linear filtering and prediction problems. *Journal of Basic Engineering*, 82(1):35–45, 1960.
 - Rudolph Emil Kalman. Mathematical description of linear dynamical systems. *Journal of the Society for Industrial and Applied Mathematics, Series A: Control*, 1(2):152–192, 1963.
 - Holger Kantz and Thomas Schreiber. *Nonlinear Time Series Analysis*. Cambridge University Press, 2004.
 - Alan A. Kaptanoglu, Brian de Silva, Ulrich Fasel, K. Kaheman, A. Goldschmidt, Jared L. Callaham, Charles B. Delahunt, Zachary Nicolaou, Kathleen P. Champion, Jean Loiseau, J. Nathan Kutz, and Steven L. Brunton. Pysindy: A comprehensive python package for robust sparse system identification. *Journal of Open Source Software*, 7(69):3994, 2022.
 - Sanjay Kowshik, Dheeraj Nagaraj, Prateek Jain, and Praneeth Netrapalli. Near-optimal offline and streaming algorithms for learning non-linear dynamical systems. In *Advances in Neural Information Processing Systems*, volume 34, pp. 8518–8531, 2021.
 - Alexander Kraskov, Harald Stögbauer, and Peter Grassberger. Estimating mutual information. *Physical Review E*, 69(6):066138, 2004.
 - William La Cava, T. R. Singh, J. Taggart, S. Suri, and Jason H. Moore. Learning concise representations for regression by evolving networks of trees. In *International Conference on Learning Representations*, 2018.
 - M. Landajuela, C. S. Lee, J. Yang, R. Glatt, C. P. Santiago, I. Aravena, T. Mundhenk, G. Mulcahy, and B. K. Petersen. A unified framework for deep symbolic regression. In *Advances in Neural Information Processing Systems*, volume 35, pp. 33985–33998, 2022.
- Zhen Liu and Milos Hauskrecht. A regularized linear dynamical system framework for multivariate time series analysis. In *Proceedings of the Twenty-Ninth AAAI Conference on Artificial Intelligence*, pp. 1798–1804, 2015.
 - Lennart Ljung. *System Identification: Theory for the User*. Prentice Hall, Upper Saddle River, NJ, 2 edition, 1999.
 - P. C. Mahalanobis. On the generalised distance in statistics. *Proceedings of the National Institute of Sciences of India*, 2:49–55, 1936.

- N. M. Mangan, J. N. Kutz, S. L. Brunton, and J. L. Proctor. Model selection for dynamical systems via sparse regression and information criteria. *Proceedings of the Royal Society A: Mathematical, Physical and Engineering Sciences*, 473(2204):20170009, 2017.
- Judea Pearl. Reverend bayes on inference engines: a distributed hierarchical approach. In *Proceedings of the Second AAAI Conference on Artificial Intelligence*, pp. 133–136, 1982.
- Yasir Sattar and Samet Oymak. Non-asymptotic and accurate learning of nonlinear dynamical systems. *Journal of Machine Learning Research*, 23(140):1–49, 2022.
- Thomas Schreiber and Andreas Schmitz. Surrogate time series. *Physica D: Nonlinear Phenomena*, 142(3–4):346–382, 2000.
- Parham Shojaee, Kaveh Meidani, Amir Barati Farimani, and Chandan Reddy. Transformer-based planning for symbolic regression. In *Advances in Neural Information Processing Systems*, volume 36, pp. 45907–45919, 2023.
- James Theiler, Stephen Eubank, André Longtin, Bryan Galdrikian, and J. Doyne Farmer. Testing for nonlinearity in time series: the method of surrogate data. *Physica D: Nonlinear Phenomena*, 58(1–4):77–94, 1992.
- Silviu-Marian Udrescu and Max Tegmark. Ai feynman: A physics-inspired method for symbolic regression. *Science Advances*, 6(16):eaay2631, 2020.
- Paul Zarchan. Fundamentals of Kalman Filtering: A Practical Approach, volume 208 of Progress in Astronautics and Aeronautics. AIAA, 2005.

A APPENDIX: NOISE NEAR STABLE PERIODIC ORBITS

We begin by examining how small random disturbances propagate when the system operates close to a stable periodic orbit. Let $f: \mathbb{R}^m \to \mathbb{R}^m$ be the state-transition map on an m-dimensional state space. Suppose $\{\mathbf{s}^{(0)}, \dots, \mathbf{s}^{(p-1)}\}$ is a p-periodic orbit, meaning the trajectory returns to its starting point after exactly p steps:

$$f(\mathbf{s}^{(k)}) = \mathbf{s}^{(k+1 \bmod p)}, \quad k = 0, \dots, p-1.$$
 (31)

This periodic sequence serves as the deterministic backbone around which noisy deviations will occur.

Linearization and monodromy. To characterize stability, we linearize the dynamics at each cycle point. Let $Df(\mathbf{s}^{(k)})$ be the Jacobian of f at $\mathbf{s}^{(k)}$, and define

$$A_k := Df(\mathbf{s}^{(k)}), \qquad M := A_{p-1} \cdots A_1 A_0,$$
 (32)

where M is the *monodromy matrix*, i.e., the linearized return map over one lap. This matrix captures how an infinitesimal perturbation transforms after completing the entire cycle.

Dynamics with noise. Now introduce noise. If $\delta_{t+k} \in \mathbb{R}^m$ is the deviation from the cycle point at time t+k, then under a small-noise approximation,

$$\delta_{t+k+1} \approx A_k \, \delta_{t+k} + \mathbf{w}_{t+k}, \qquad k = 0, \dots, p-1, \tag{33}$$

where \mathbf{w}_{t+k} is an additive zero-mean disturbance with covariance $\Sigma_k = \operatorname{Cov}(\mathbf{w}_{t+k})$. Aggregating one lap gives

$$\delta_{t+p} \approx M \, \delta_t + \bar{\mathbf{w}}_t, \tag{34}$$

where the effective disturbance is the weighted sum

$$\bar{\mathbf{w}}_{t} = \sum_{k=0}^{p-1} \left(A_{p-1} \cdots A_{k+1} \right) \mathbf{w}_{t+k}, \tag{35}$$

with covariance

$$\bar{\Sigma} = \sum_{k=0}^{p-1} (A_{p-1} \cdots A_{k+1}) \, \Sigma_k \, (A_{p-1} \cdots A_{k+1})^\top.$$
 (36)

Long-run covariance. Define $Q_n := \text{Cov}(\delta_{t+pn})$, the deviation covariance sampled once per lap. It obeys the Lyapunov recursion

$$Q_{n+1} = M Q_n M^{\top} + \bar{\Sigma}. \tag{37}$$

If the spectral radius $\rho(M) < 1$ (all eigenvalues inside the unit disk), this recursion converges to the unique positive semidefinite fixed point

$$Q_{\star} = \sum_{j=0}^{\infty} M^j \,\bar{\Sigma} \,(M^{\top})^j. \tag{38}$$

Hence near a stable periodic orbit, noise is continually damped by the cycle, and the system fluctuates with finite variance around the orbit.

B APPENDIX: DETAILS ON CONDITIONAL MUTUAL INFORMATION FOR MARKOV ORDER

This appendix provides a detailed account of how conditional mutual information (CMI) is used to initialize the Markov order p_0 .

B.1 DEFINITION

Mutual information (MI) between two random variables X and Y measures their statistical dependence:

$$I(X;Y) = \int p(x,y) \log \frac{p(x,y)}{p(x)p(y)} dx dy.$$

It vanishes if and only if *X* and *Y* are independent.

The *conditional* mutual information generalizes this notion: for random variables (X, Y, Z),

$$I(X;Y \mid Z) \; = \; \int p(x,y,z) \log \frac{p(x,y \mid z)}{p(x \mid z)p(y \mid z)} \, dx \, dy \, dz.$$

Here $I(X; Y \mid Z) = 0$ means that once Z is known, X provides no further information about Y.

B.2 APPLICATION TO MARKOV ORDER

Given a univariate time series $\{y_t\}$, we test whether lag p contributes predictive information beyond more recent lags. This is formalized by

$$I(y_t; y_{t-p} | y_{t-1}, \dots, y_{t-p+1}).$$

If this conditional mutual information vanishes, then y_{t-p} is redundant given the last p-1 observations. The true Markov order is the largest lag p for which the above quantity is nonzero.

B.3 ESTIMATION

In practice, CMI must be estimated from finite samples. We employ nonparametric, near-est-neighbor-based estimators such as the k-nearest-neighbor method of Kraskov et al. (2004) and its conditional extension (Frenzel & Pompe, 2007). These estimators approximate local densities by distances to neighboring points in the joint space, avoiding explicit kernel bandwidth selection and adapting naturally to different scales.

Formally, one computes

$$\widehat{I}(X;Y\mid Z) \ = \ \psi(k) + \frac{1}{N} \sum_{i=1}^{N} \left[\psi(n_{z}^{(i)}) - \psi(n_{xz}^{(i)}) - \psi(n_{yz}^{(i)}) \right],$$

where ψ is the digamma function, $n_z^{(i)}$ counts neighbors of sample i in the Z-space, and $n_{xz}^{(i)}, n_{yz}^{(i)}$ count neighbors in the joint spaces (X,Z) and (Y,Z). Intuitively, larger CMI values correspond to stronger predictive influence of the lagged variable.

B.4 SIGNIFICANCE TESTING

Because sampling noise ensures $\hat{I} > 0$ even for irrelevant lags, we use surrogate testing to separate signal from noise. Specifically:

1. Fix lag p and compute the observed statistic \widehat{I}_{obs} . 2. Generate B surrogate series by randomly permuting y_{t-p} across time, which destroys temporal dependence but preserves the marginal distribution. 3. Recompute $\widehat{I}^{(b)}$ on each surrogate, forming a null distribution. 4. Compute the p-value

$$q_p = \frac{1}{B} \sum_{b=1}^{B} \mathbf{1} \{ \hat{I}^{(b)} \ge \hat{I}_{\text{obs}} \}.$$

5. Declare lag p significant if $q_p < \alpha$ (typically $\alpha = 0.05$).

The initialization is then defined as

$$p_0 = \max\{p: q_p < \alpha\},\$$

the longest lag whose incremental information passes significance testing. This provides a robust, interpretable proxy for the effective memory length of the observed process.

C APPENDIX: STABILITY PROXIMITY METRICS AND FILTER SELECTION

This appendix expands on the stability-proximity assessment used to guide filter selection.

Rolling mean and covariance. Given observations $\{y_t\}_{t=1}^T \subset \mathbb{R}^d$ and a window size W, we form overlapping segments [t, t+W-1] with rolling mean μ_t and covariance C_t as in equation 19. These provide local estimates of central tendency and dispersion.

Baseline normalization. To make quantities comparable across windows, we anchor statistics to a baseline taken from the first $L_0 = \max\{10, |\sqrt{T}|\}$ samples:

$$\mu_0 = \frac{1}{L_0} \sum_{i=1}^{L_0} y_i, \qquad S_0 = \text{Cov}(y_{1:L_0}) + \epsilon I_d.$$

Here S_0 is used as a reference covariance to normalize subsequent deviations.

Scalar proxies. We reduce the rolling statistics to two univariate time series:

$$m_t = (\mu_t - \mu_0)^{\top} S_0^{-1} (\mu_t - \mu_0),$$
 (39)

$$v_t = \log \det(C_t + \epsilon I_d). \tag{40}$$

The first measures the Mahalanobis distance of the local mean from baseline; the second measures the log-volume of the covariance ellipsoid. Together they reflect mean drift and variance contraction.

Tail metrics. Since transient fluctuations are expected, we examine only the last fraction of each proxy sequence (the "tail"), which better reflects steady–state behavior. For a scalar series z_1,\ldots,z_n , let the final $L=\lceil \alpha n \rceil$ values form the tail (typically $\alpha=0.4$). Two robust statistics are then computed: - *Drift index D* via the Theil–Sen slope estimator ?:

$$D = \frac{|\operatorname{median}_{i < j}(z_j - z_i)/(j - i)| \cdot L}{\operatorname{IQR}(\operatorname{tail}) + \epsilon},$$

which measures normalized monotonic trend in the tail. - $Reduction\ index\ R$ given by the ratio of dispersion in the tail relative to the full sequence:

$$R = \frac{\mathrm{IQR}(\mathrm{tail})}{\mathrm{IQR}(\mathrm{full}) + \epsilon}.$$

Here IQR denotes the interquartile range. Intuitively, D quantifies whether the proxy is still trending, and R whether variability has shrunk.

Multivariate combination. The two proxies m_t and v_t each yield (D, R) pairs. To combine them, we take

$$D_{\text{max}} = \max(D_m, D_v), \qquad R_{\text{max}} = \max(R_m, R_v), \qquad S = D_{\text{max}} + \alpha R_{\text{max}},$$

with α a weight (default $\alpha = 1$). This ensures conservativeness: instability in either channel marks the system as far from equilibrium.

Classification and filter choice. Thresholds on $(D_{\text{max}}, R_{\text{max}})$ determine stability classes:

$$\text{Near: } D_{\max} \leq \tau_{\text{near}}^D, \ \ R_{\max} \leq \tau_{\text{near}}^R; \quad \text{Transition: } D_{\max} \leq \tau_{\text{trans}}^D, \ \ R_{\max} \leq \tau_{\text{trans}}^R; \quad \text{otherwise: Far.}$$

- *Near*: statistics have converged, indicating proximity to an attractor. The system is effectively linearized, so an EKF suffices. - *Transition*: contraction is partial, suggesting intermittent nonlinear excursions. Both EKF and PF are viable; we allow either. - *Far*: proxies fluctuate strongly, signaling nonlinearity and poor contraction. PF is chosen for robustness.

Window selection. Choosing W is critical: too small leads to noise, too large washes out local dynamics. We suggest candidates using \sqrt{T} , fixed grids, FFT-detected dominant periods, or external hints (e.g. Markov order). The final window is selected by minimizing the score S.

D APPENDIX: DETAILED PROCEDURE FOR INFERENCE AND LEARNING

This appendix expands the inner loop for a fixed structure (p,m), where p is the Markov order and m the observation dimension. We work with the augmented first-order model in Eqs. equation 23-equation 24. At each iteration we alternate between:

- Inference (E-step): estimate the latent augmented trajectory $\{\mathbf{x}_t\}_{t=1}^N$ and its posterior moments under the current parameters Θ ;
- Learning (M-step): update Θ by minimizing the expected negative log-likelihood (the EM Q-function) plus a structural regularizer.

A. AUGMENTED FORMULATION AND FEATURES

Let k be the intrinsic latent dimension; the augmented state stacks p consecutive latent vectors, so $\mathbf{x}_t \in \mathbb{R}^{k_{\mathrm{aug}}}$ with $k_{\mathrm{aug}} = kp$. The top k coordinates evolve nonlinearly via a polynomial feature map of degrees 1:o; the lower blocks implement the (p-1)-step shift. Writing $\phi_{\mathrm{aug}}(\mathbf{x}_t) \in \mathbb{R}^F$ for the monomial dictionary (including degree 1 terms), the dynamics and observations are:

$$\mathbf{x}_{t+1} = \mathbf{b}_{\text{aug}} + A_{\text{aug}} \phi_{\text{aug}}(\mathbf{x}_t) + \mathbf{w}_t, \quad \mathbf{y}_t = C_{\text{aug}} \mathbf{x}_t + \mathbf{d} + \mathbf{v}_t,$$

with Gaussian noises $\mathbf{w}_t \sim \mathcal{N}(\mathbf{0}, (\Sigma_w)_{\mathrm{aug}})$, $\mathbf{v}_t \sim \mathcal{N}(\mathbf{0}, \Sigma_v)$. The block structure of $(\mathbf{b}_{\mathrm{aug}}, A_{\mathrm{aug}}, C_{\mathrm{aug}})$ encodes "nonlinear top block + shift," so that higher-order (in p) dynamics are handled by first-order filtering in the augmented space.

Posterior objects we need. The learning step only requires a small set of sufficient statistics, collectively denoted

$$\mathcal{M} = \left\{ \mathbb{E}[\mathbf{x}_t], \ \mathbb{E}[\mathbf{x}_t \mathbf{x}_t^\top], \ \mathbb{E}[\mathbf{x}_{t+1} \mathbf{x}_t^\top], \ \mathbb{E}[\Phi(\mathbf{x}_t)], \ \mathbb{E}[\Phi(\mathbf{x}_t) \Phi(\mathbf{x}_t)^\top], \ \mathbb{E}[\mathbf{x}_{t+1} \Phi(\mathbf{x}_t)^\top] \right\}_{t=1}^N,$$

where $\Phi(\mathbf{x}_t)$ concatenates the degree-1 coordinates and the higher-order polynomial features used by the transition map. The E-step (filtering) produces numerical approximations of these moments.

B. Inference: Two complementary filters

We adopt a data-driven stability classifier (rolling window) that labels local regimes as *near/transition* or *far*. Intuitively, when the local linearization is accurate and innovations are close to Gaussian, an EKF is effective; otherwise we resort to a particle filter (PF). Both operate in the augmented state.

B.1 Extended Kalman Filter (EKF) Kalman (1960). The EKF linearizes the nonlinear transition at the current mean. Let $\hat{\mathbf{x}}_{t|t}$ be the filtered mean and $P_{t|t}$ its covariance at time t. The prediction step forms

$$\widehat{\mathbf{x}}_{t+1|t} = \mathbf{b}_{\mathrm{aug}} + A_{\mathrm{aug}} \, \phi_{\mathrm{aug}}(\widehat{\mathbf{x}}_{t|t}), \qquad P_{t+1|t} = J_t P_{t|t} J_t^\top + (\Sigma_w)_{\mathrm{aug}},$$

where J_t is the Jacobian of the transition map evaluated at $\hat{\mathbf{x}}_{t|t}$ (its top $k \times k_{\text{aug}}$ block comes from the polynomial map's analytic Jacobian; the lower blocks are shift identities). The update step uses the innovation

$$\mathbf{r}_t = \mathbf{y}_t - (C_{\text{aug}} \widehat{\mathbf{x}}_{t|t-1} + \mathbf{d}), \qquad S_t = C_{\text{aug}} P_{t|t-1} C_{\text{aug}}^{\top} + \Sigma_v,$$

and the Kalman gain $K_t = P_{t|t-1}C_{\text{aug}}^{\top}S_t^{-1}$ to obtain

$$\widehat{\mathbf{x}}_{t|t} = \widehat{\mathbf{x}}_{t|t-1} + K_t \mathbf{r}_t, \qquad P_{t|t} = (I - K_t C_{\text{aug}}) P_{t|t-1} (I - K_t C_{\text{aug}})^\top + K_t \Sigma_v K_t^\top.$$

Intuition. EKF replaces the nonlinear dynamics by their best local linear approximation around the current estimate. It is accurate when the state stays in a region where the linearization error is small (near equilibria or along gently curved manifolds).

B.2 Bootstrap Particle Filter (PF) Gordon et al. (1993). When the system is far from equilibrium or the noise departs from Gaussianity, we approximate the posterior by a set of weighted particles. Using the transition prior as proposal, the recursion is:

- 1. *Propagation:* for each particle i, sample $\mathbf{x}_t^{(i)} \sim p(\mathbf{x}_t \mid \mathbf{x}_{t-1}^{(i)})$ using the nonlinear transition.
- 2. Weighting: update $w_t^{(i)} \propto w_{t-1}^{(i)} p(\mathbf{y}_t \mid \mathbf{x}_t^{(i)})$, where $p(\mathbf{y}_t \mid \mathbf{x}_t^{(i)})$ is Gaussian under the linear observation model.
- 3. Normalization and resampling: normalize $\{w_t^{(i)}\}$; if the effective sample size $\mathrm{ESS}_t = 1/\sum_i (w_t^{(i)})^2$ falls below a threshold, resample (e.g., systematic resampling) to prevent weight degeneracy.

Posterior means/covariances are approximated by weighted averages over particles (e.g., $\mathbb{E}[\mathbf{x}_t] \approx \sum_i w_t^{(i)} \mathbf{x}_t^{(i)}$). Cross-moments such as $\mathbb{E}[\mathbf{x}_{t+1}\mathbf{x}_t^{\top}]$ are formed by tracking particle ancestry (pair each $\mathbf{x}_{t+1}^{(i)}$ with its parent $\mathbf{x}_t^{(a(i))}$ and average with weights). *Intuition*. PF keeps the nonlinear geometry intact: particles follow the true dynamics, so highly non-Gaussian or multimodal posteriors can be represented.

B.3 Log-likelihood and moments. Both filters provide an estimate of the marginal log-likelihood $\log p(\mathbf{Y} \mid \Theta)$ (EKF via Gaussian innovations; PF via log-mean-exp of weights) and the posterior set \mathcal{M} . The latter supplies all expectations needed by the learning step.

C. LEARNING VIA THE EM Q-FUNCTION

Let $S = \{x_t\}$ denote the latent trajectory. The EM auxiliary function is the posterior expectation of the complete-data negative log-likelihood (plus regularization):

$$\min_{\Theta} Q(\mathbf{Y}, \mathcal{S}, \Theta) + r(A_{\text{top}}), \quad Q = \mathbb{E} \left[\sum_{t=1}^{N} \mathcal{D}(\mathbf{y}_{t}, C_{\text{aug}}\mathbf{x}_{t} + \mathbf{d}, \Sigma_{v}) + \sum_{t=1}^{N-1} \mathcal{D}(\mathbf{x}_{t+1}, \mathbf{b}_{\text{aug}} + A_{\text{aug}}\phi_{\text{aug}}(\mathbf{x}_{t}), \Sigma_{w}) \right],$$

where $\mathcal{D}(\mathbf{u}, \mathbf{v}, \Sigma) = (\mathbf{u} - \mathbf{v})^{\top} \Sigma^{-1} (\mathbf{u} - \mathbf{v})$ is the squared Mahalanobis distance.

C.1 Transition update (top block). Because the augmented transition has the "nonlinear top + shift" structure, the parameters to learn are the top-block bias b and matrix A_{top} in

$$\mathbf{x}_{t+1}^{\text{top}} \approx \mathbf{b} + A_{\text{top}} \Phi(\mathbf{x}_t).$$

Taking expectations under the posterior, the transition part of Q reduces to a regularized multivariate regression with design matrix built from $\mathbb{E}[\Phi(\mathbf{x}_t)]$ and Gram/cross-moments $\mathbb{E}[\Phi(\mathbf{x}_t)\Phi(\mathbf{x}_t)^{\top}]$, $\mathbb{E}[\mathbf{x}_{t+1}^{\text{top}}\Phi(\mathbf{x}_t)^{\top}]$. Writing $Z_t = \Phi(\mathbf{x}_t)$ and $Y_t = \mathbf{x}_{t+1}^{\text{top}}$, the normal-equation form is

$$\min_{\mathbf{b}, A_{\text{top}}} \sum_{t} \| Y_t - \mathbf{b} - A_{\text{top}} Z_t \|_{\Sigma_w^{-1}}^2 + r(A_{\text{top}}),$$

where $\|\mathbf{u}\|_{\Sigma^{-1}}^2 = \mathbf{u}^{\top} \Sigma^{-1} \mathbf{u}$. The regularizer

$$r(A_{\text{top}}) = \frac{\lambda_2}{2} \|A_{\text{top}} - A_{\text{id}}\|_F^2 + \lambda_1 \|A_{\text{top}} - A_{\text{id}}\|_1$$

biases degree–1 coefficients toward identity (stability/interpretability) while encouraging sparsity in higher-order terms. With $\lambda_1=0$ this yields a closed-form ridge update using the sufficient statistics of Z_t ; **b** is updated by the mean residual.

- **C.2 Observation update.** If C_{aug} is to be estimated, the observation term in Q similarly becomes a weighted least-squares problem in C_{aug} (and d) based on $\{\mathbb{E}[\mathbf{x}_t], \mathbb{E}[\mathbf{x}_t\mathbf{x}_t^{\top}]\}$. In our main experiments we either hold C_{aug} fixed or update it conservatively to avoid overfitting.
- **C.3 Noise covariances.** The Gaussian covariances $(\Sigma_w)_{\text{aug}}, \Sigma_v$ can be held fixed for robustness, or re-estimated in closed form by matching posterior quadratic forms (standard in linear-Gaussian EM). Re-estimation is optional and not critical to the structural conclusions.

D. EM ALTERNATION AND STOPPING

One inner-loop cycle is:

- 1. **E-step:** run EKF or PF on the augmented model to obtain \mathcal{M} and the marginal log-likelihood log $p(\mathbf{Y} \mid \Theta)$;
- 2. **M-step:** update $\{\mathbf{b}, A_{\text{top}}\}$ (and optionally C_{aug}) by minimizing Q+r using the posterior moments.

Under exact E/M steps the EM objective decreases monotonically Dempster et al. (1977); with EKF/PF approximations we monitor the composite loss $\mathcal{L}(\Theta) = -\log p(\mathbf{Y} \mid \Theta) + r(A_{\text{top}})$ and stop when its relative decrease falls below a tolerance or a maximum number of iterations is reached.

E APPENDIX: SELF-DESIGNED DYNAMICAL SYSTEMS

To complement canonical benchmarks, we designed a small suite of nonlinear dynamical systems that exhibit higher–order dependencies and non-polynomial nonlinearities. Each system is specified by an explicit recurrence with tunable parameters. Unless otherwise noted, $\{s_t\}$ denotes the latent state, and (x_t, y_t, z_t) its components.

1. Exponential-logarithmic 2D system (p = 2). This model mixes exponential suppression, logarithmic growth, and bounded bilinear coupling:

$$x_{t+1} = ax_t + bx_{t-1} + c\left(e^{-y_t^2} - e^{-x_t^2}\right) + d\log(1+y_t^2) - e\frac{x_t y_t}{1+x_t^2 + y_t^2},$$

$$y_{t+1} = ay_t + by_{t-1} + c\left(e^{-x_t^2} - e^{-y_t^2}\right) + d\log(1+x_t^2) - e\frac{x_t y_t}{1+x_t^2 + y_t^2}.$$

2. Logistic 2D system (p = 3). Centered logistic couplings with nonlinear damping:

$$x_{t+1} = a_1 x_t + a_2 x_{t-1} + a_3 x_{t-2} + \beta \sigma(y_t) - g \frac{x_t^3}{1 + x_t^2},$$

$$y_{t+1} = a_1 y_t + a_2 y_{t-1} + a_3 y_{t-2} + \beta \sigma(x_t) - g \frac{y_t^3}{1 + y_t^2},$$

where $\sigma(z) = \frac{1}{1+e^{-z}} - \frac{1}{2}$ is a centered logistic function.

3. Soft ring 3D system (p=2). Variables interact in a cyclic fashion via a smooth contrast function ϕ_{soft} :

$$\begin{aligned} x_{t+1} &= ax_t + bx_{t-1} + e \,\phi_{\text{soft}}(y_t, z_t), \\ y_{t+1} &= ay_t + by_{t-1} + e \,\phi_{\text{soft}}(z_t, x_t), \\ z_{t+1} &= az_t + bz_{t-1} + e \,\phi_{\text{soft}}(x_t, y_t). \end{aligned}$$

4. Simple exponential 2D system (p = 2)**.** Minimal design with exponential cross-suppression:

$$x_{t+1} = ax_t + bx_{t-1} + ce^{-y_t^2}, y_{t+1} = ay_t + by_{t-1} + ce^{-x_t^2}.$$

5. Log-ratio 3D system (p = 2). Each coordinate updates with a log-difference structure:

$$x_{t+1} = ax_t + bx_{t-1} + c\log(1 + y_t^2) - d\log(1 + z_t^2),$$

$$y_{t+1} = ay_t + by_{t-1} + c\log(1 + z_t^2) - d\log(1 + x_t^2),$$

$$z_{t+1} = az_t + bz_{t-1} + c\log(1 + x_t^2) - d\log(1 + y_t^2).$$

6. Tri-gate 2D system (p = 2)**.** Asymmetric gating, where x is self-damped and y is one-way gated by x:

$$x_{t+1} = a_x x_t + b_x x_{t-1} - c_x x_t^3,$$

$$y_{t+1} = a_y y_t + b_y y_{t-1} + g_y e^{-x_t^2}.$$

7. Leaky-log 2D system (p = 2)**.** A compact model where y ignores its past but responds logarithmically to x:

$$x_{t+1} = a_x x_t + b_x x_{t-1}, y_{t+1} = r_y y_t + g_y \log(1 + x_t^2).$$

8. Chain 3D system (p = 2). A one-way cascade $x \to y \to z$:

$$x_{t+1} = a_x x_t + b_x x_{t-1} - d_x x_t^3,$$

$$y_{t+1} = a_y y_t + b_y y_{t-1} + e_1 e^{-x_t^2},$$

$$z_{t+1} = a_z z_t + b_z z_{t-1} + e_2 \log(1 + y_t^2).$$

These designs illustrate qualitatively distinct nonlinear behaviors: saturation (logistic), suppression (exponential), long-memory polynomial damping, and asymmetric gating. All remain polynomial-or log/exp-modulated, ensuring stability of numerical simulation while challenging inference due to non-polynomial nonlinearities.